

Supporting Information

Ultra-thick electrodes based on activated wood-carbon toward high-performance quasi-solid-state supercapacitors

Wenjia Zhang,^a Ting Liu,^a Jirong Mou,^a Jianlin Huang,^{*a} and Meilin Liu^b

^aGuangzhou Key Laboratory for Surface Chemistry of Energy Materials, New Energy Institute, School of Environment and Energy, South China University of Technology, Guangzhou 510006, China.

^bA Materials Science and Engineering, Georgia Institute of Technology, Address, Atlanta, GA 30332-0245, USA.

Additional images



Figure S1. Construction of a quasi-solid-state symmetric supercapacitor (SSC) based on activated wood carbon (AWC) monoliths as freestanding thick electrodes.

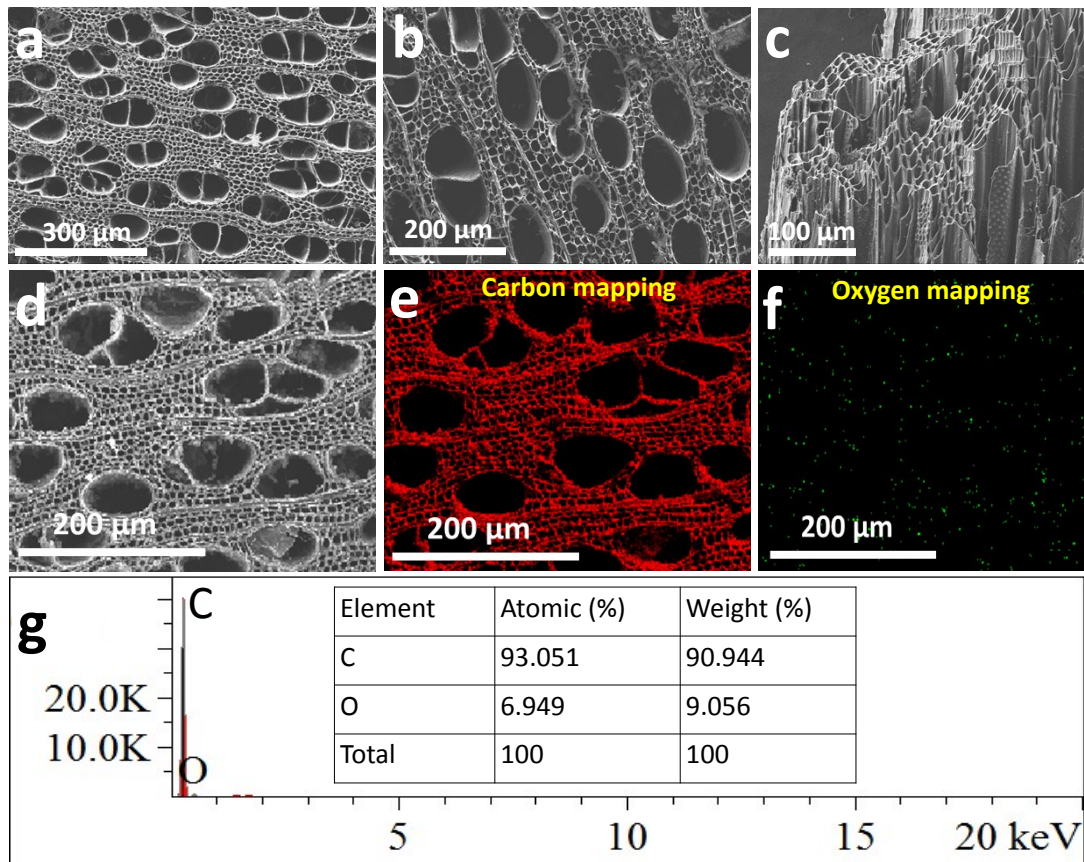


Figure S2. (a-d) SEM images for the carbonized wood (CW), and e, f) Elemental mapping images of e) C and f) O, respectively in (d). (g) the atomic ratio of C and O in the CW.

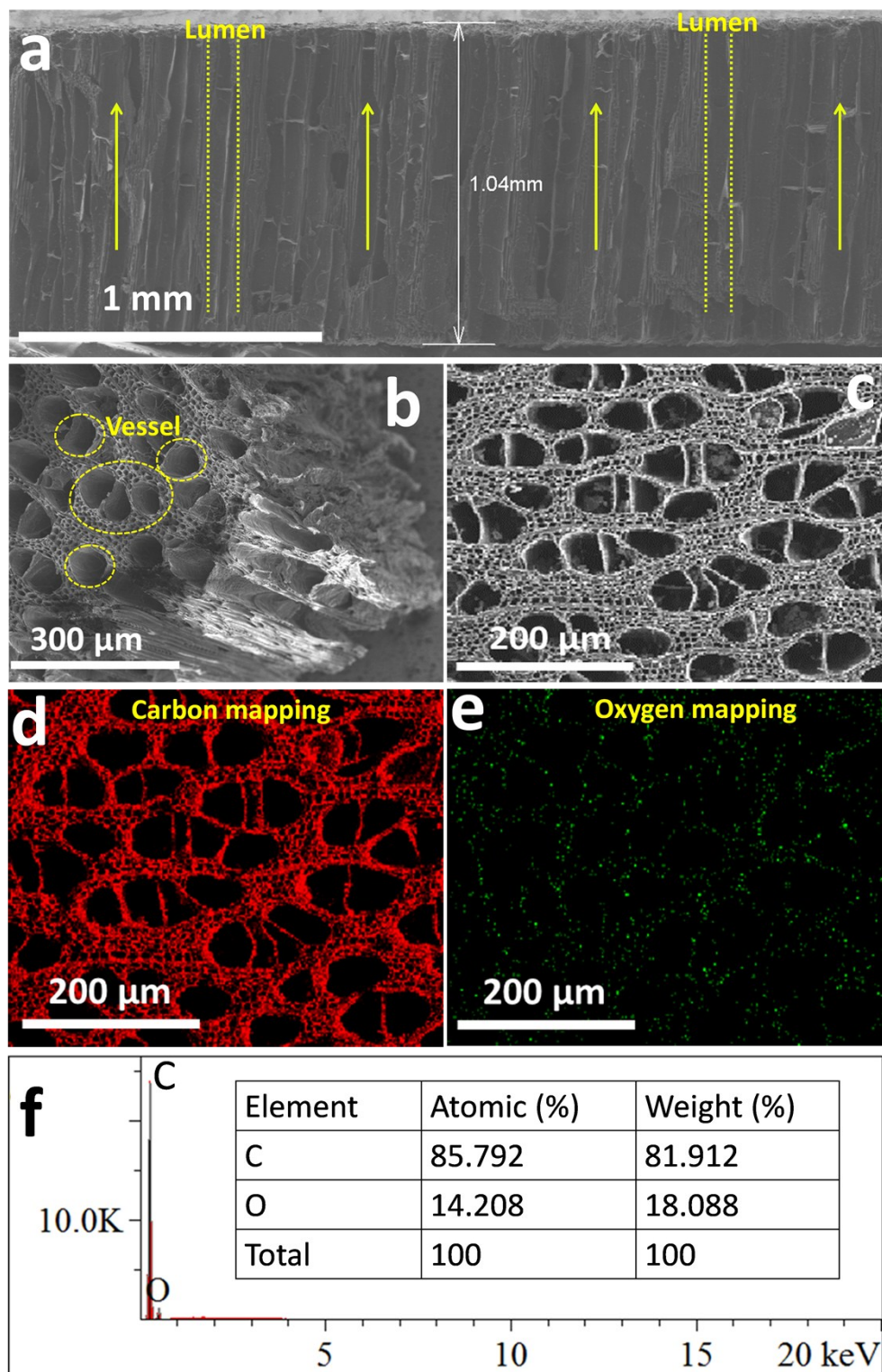


Figure S3. (a-c) SEM images for the activated wood carbon (AWC): a) cross-sectional view, showing the thickness of 1.04 mm for the AWC; b, c) top view; (d, e) Elemental mapping images of i) C and j) O, respectively in (c). (f) the atomic ratio of C and O in the AWC.

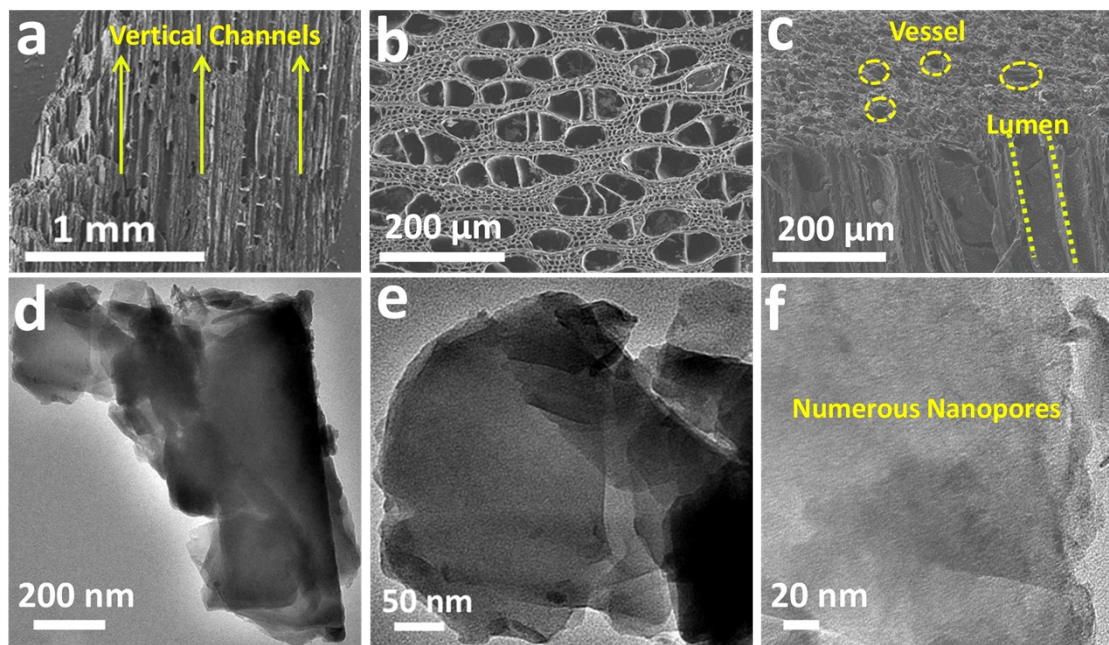


Figure S4. (a-c) SEM images for the activated wood carbon (AWC), showing numerous vertical channels in the AWC; d-f) different magnification TEM images of the AWC, demonstrating highly nanoporous structure.

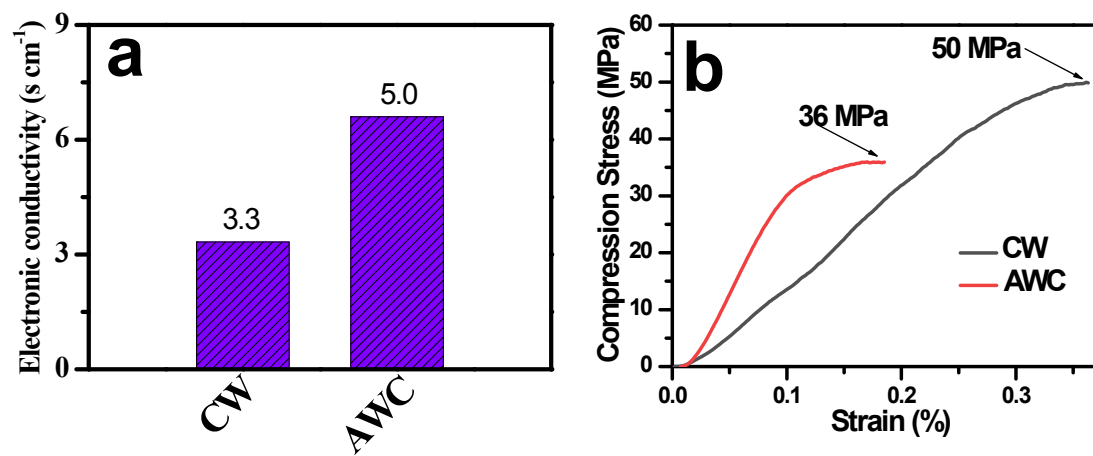


Figure S5. Electrical and mechanical properties of the CW and AWC electrodes: (a) electronic conductivity, (b) compressive stress-strain curves.

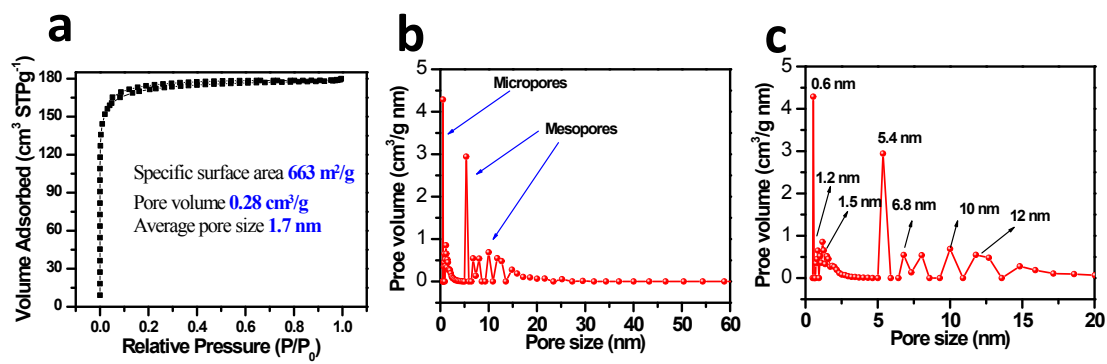


Figure S6. The analysis on hierarchical porous structure in the activated wood carbon (AWC), (a) N_2 adsorption and desorption isotherm; and (b) pore size distribution; (c) a part of 0-20 nm pore size magnified in (b).

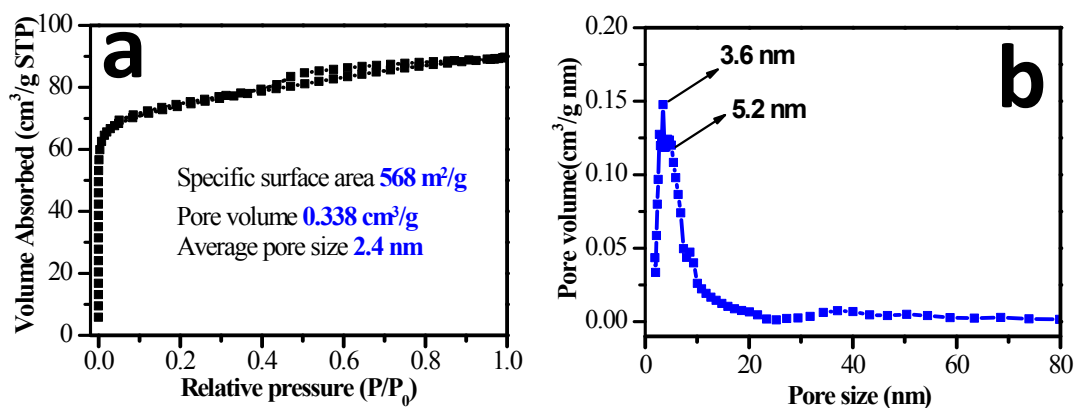


Figure S7. The analysis on porous structure in the carbonized wood (CW), (a) N_2 adsorption and desorption isotherm; and (b) pore size distribution.

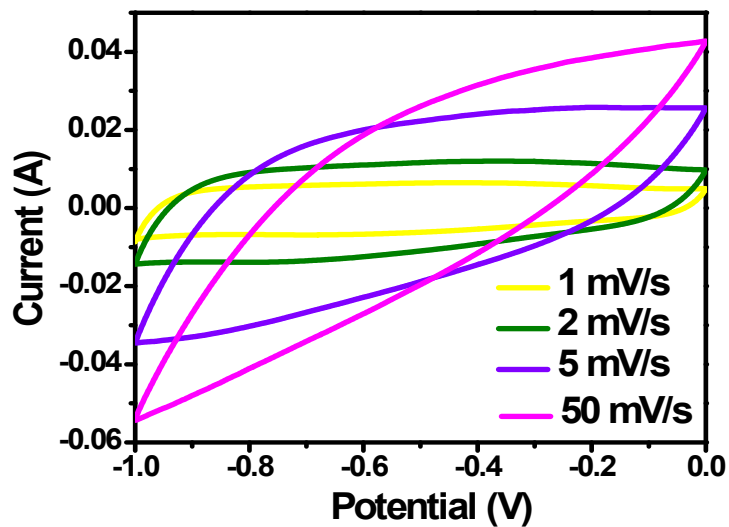


Figure S8. CV curves of the AWC electrode at the scan rate from 1.0 to 50 mV/s.

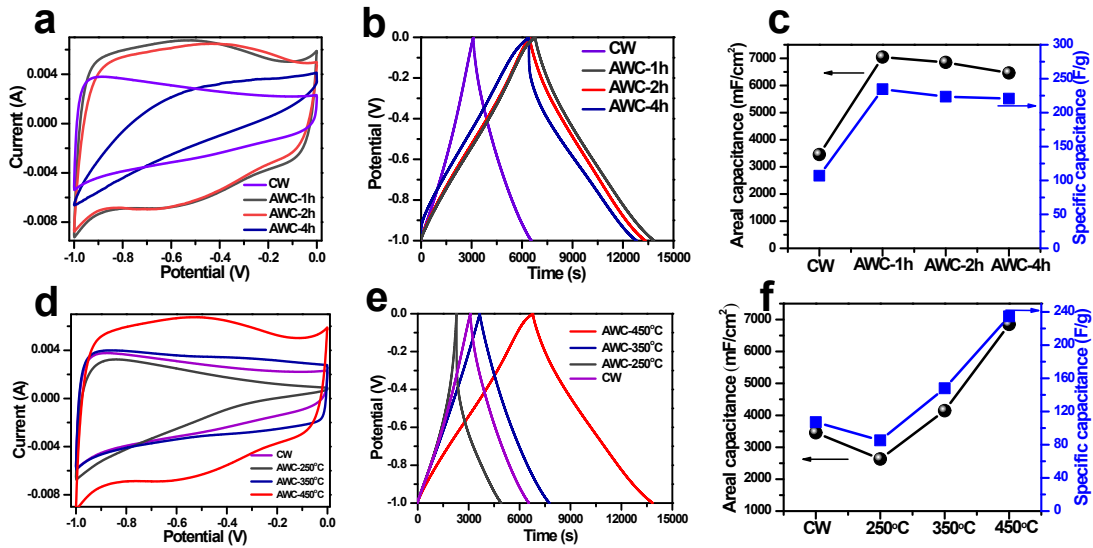


Figure S9. The electrochemical performance of the AWC samples with different activation time (a-c) and temperature (d-f) in air atmosphere; (a, d) CV curves at the scan rate of 1.0 mV/s, (b, e) galvanostatic charge-discharge curves at a current densities of 1.0 mA/cm²; and (c, f) specific capacitance. When the activation time was increased from 1 to 4 hours, the capacitance value exhibits a slight decrease. However, the activation temperature was increased from 250 to 450°C, the capacitance value exhibits an obvious increase, further increasing the activation temperature (above 450°C), the AWC sample will be gone by burning. Hence, the activation time and temperature of 1h and 450°C respectively are the best condition.

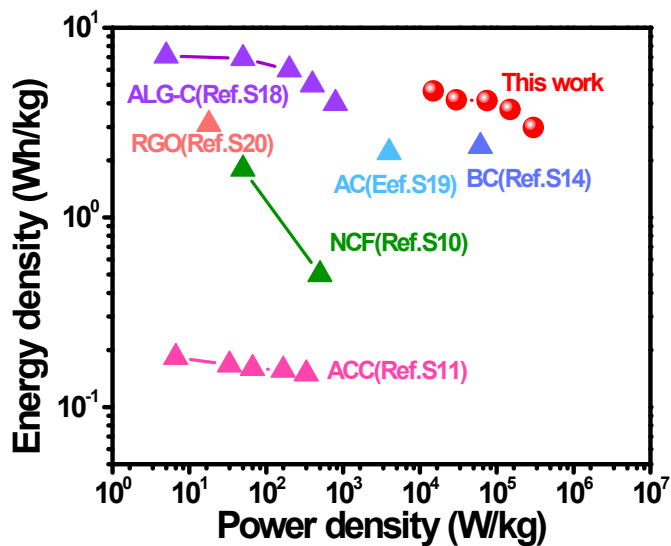


Figure S10. Comparison of the energy and power densities based mass of the two electrodes with the previously reported electrode materials.

In addition, the quasi-solid-state SSC also demonstrated an increased energy density of 4.64 Wh/kg at a power density of 14.95 kW/kg, showing better performance than some carbon-based supercapacitors reported recently.



Figure S11. The quasi-solid-state SSC assembled by the two identical AWC powered an LED (1 W) for 10 mins by three in series.

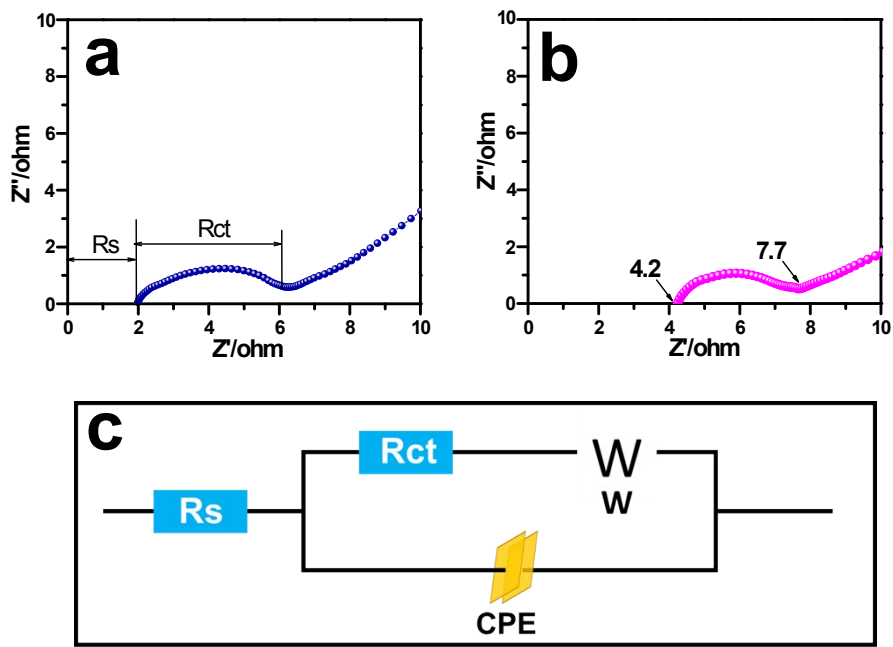


Figure S12. Electrochemical impedance spectra of AWC electrode; (a) in liquid electrolyte, (b) quasi-solid-state SSC, and (c) the equivalent circuit used to model the impedance data.

Table S1. Comparison of electrochemical performance of AWC thick electrode with some representative porous carbon-based electrodes recently reported for supercapacitors.

Electrode material	Test system	Cycles/retention	Specific capacitances	Ref.
Graphene-PANI/Graphene	3-electrode	5000/95%	190.6 mF/cm ² 0.5 mA/cm ²	1
CTAs@NCB-700 (T)	3-electrode	10000/98%	366 mF/cm ² 1 mA/cm ²	2
CNT/PPy	3-electrode	10000/95%	280 mF/cm ² , 1.4 mA/cm ²	3
Graphene/PANI-paper	3-electrode	10000/83%	335 mF/cm ² , 0.5 mA/cm ²	4
CNFs	2-electrode	/	144 F/g, 0.5 A/g	5
Oxygen-deficient Fe ₂ O ₃	3-electrode	10000/95.2%	382.7 mF/cm ² , 0.5 mA/cm ²	6
HPNC	3-electrode	5000/81%	172 F/g, 0.1 A/g	7
MnO ₂ /ZnO//RGO	3-electrode	/	230 mF/cm ² , 10 mV/s	8
MVNN-CNT	3-electrode	/	178 mF/cm ² , 1.1 mA/cm ²	9
NCF	3-electrode	1000/95.8%	332 mF/cm ² 1 mA/cm ²	10
ACC	3-electrode	20000/97%	88 mF/cm ² 10 mV/s	11
LSG-EC	3-electrode	10000/96.5%	3.67 mF/cm ² 1 A/g	12
AWC	3-electrode	10000/96%	235 F/g, 6850 mF/cm ² , 1 mA/cm ²	<i>This work</i>

Table S2: Volumetric capacitance and energy density comparison of the AWC thick electrode and some representative carbon-/metal oxide-based electrodes at device level.

Electrode material	Volumetric capacitance	Volumetric Energy density (mW h cm ⁻³)	Cycles/retention	Specific capacitances	Ref.
Graphene/PANI-paper	3.55 F/cm ³ , 4.57 mA/cm ³	0.32 mW h/cm ³ , 540 mW/cm ³	10000/ 83%	77.8 mF/cm ² 0.1 mA/cm ²	4
Oxygen-deficient Fe ₂ O ₃	1.21 F/cm ³ , 0.5 mA/cm ³	0.41 mW h/cm ³ , 100 mW/cm ³	6000/ 81.6%	382.7 mF/cm ² 0.5 mA/cm ²	6
MnO ₂ /ZnO//RGO	0.52 F/cm ³ , 10 mV/s	0.234 mW h/cm ³ , 133 mW/cm ³	5000/ 98.4%	250 mF/cm ² , 10 mV/s	8
NCF	0.132 F/cm ³ , 1 mA/cm ²	0.018 mW h/cm ³ , 1.8mW/cm ³	4000/ 96%	/	10
ACC	0.067 F/cm ³ , 10 mV/s	0.055 mW h/cm ³ , 2 mW/cm ³	20000/ 95%	31 mF/cm ³ , 10 mV/s	11
LSG	0.003 F/cm ³ , 10 mA/cm ³	1.36 mW h/cm ³ , 20 mW/cm ³	10000/ 97%	/	12
MnO ₂ /C	2.5 F/cm ³ , 20 V/s	0.12 mW h/cm ³ , 400 mW/cm ³	10000/ 84%	/	13
BC	2.1 F/cm ³ , 33 mA/cm ³	0.24 mW h/cm ³ , 6100 mW/cm ³	10000/ 96%	/	14
CoP/MnO ₂ /CC	1.94 F/cm ³ , 1 mA/cm ³	0.69 mW h/cm ³ , 114.2 mW/cm ³	5000/ 82%	571.3 mF/cm ² , 1 mA/cm ²	15
Fe ₂ O ₃ /MnO ₂	1.5 F/cm ³ , 2 mA/cm ³	0.55 mW h/cm ³ , 139.1 mW/cm ³	5000/ 84%	180.4 mF/cm ² , 1 mA/cm ²	16
Ni(OH) ₂ //Mn ₃ O ₄	2.07 F/cm ³ , 1 mA/cm ³	0.35 mW h/cm ³ , 32.5 mW/cm ³	12000/ 83.3%	372.5 mF/cm ² , 1 mA/cm ²	17
AWC	5.58 F/cm ³ 3.3 mA/cm ³	0.77 mW h cm ⁻³ 2500 mWcm ⁻³	10000/ 86%	33.5 F/g, 1675 mF/cm ² , 1 mA/cm ²	This work

References

1. Chi, K.; Zhang, Z.; Xi, J.; Huang, Y.; Xiao, F.; Wang, S.; Liu, Y., Freestanding graphene paper supported three-dimensional porous graphene-polyaniline nanocomposite synthesized by inkjet printing and in flexible all-solid-state supercapacitor. *ACS Appl. Mater. Interfaces* **2014**, *6* (18), 16312-9.
2. Tang, Z.; Zhang, G.; Zhang, H.; Wang, L.; Shi, H.; Wei, D.; Duan, H., MOF-derived N-doped carbon bubbles on carbon tube arrays for flexible high-rate supercapacitors. *Energy Storage Mater.* **2018**, *10*, 75-84.
3. Chen, Y.; Du, L.; Yang, P.; Sun, P.; Yu, X.; Mai, W., Significantly enhanced robustness and electrochemical performance of flexible carbon nanotube-based supercapacitors by electrodepositing polypyrrole. *J. Power Sources* **2015**, *287*, 68-74.
4. Yao, B.; Yuan, L.; Xiao, X.; Zhang, J.; Qi, Y.; Zhou, J.; Zhou, J.; Hu, B.; Chen, W., Paper-based solid-state supercapacitors with pencil-drawing graphite/polyaniline networks hybrid electrodes. *Nano Energy* **2013**, *2* (6), 1071-1078.
5. Li, S. C.; Hu, B. C.; Ding, Y. W.; Liang, H. W.; Li, C.; Yu, Z. Y.; Wu, Z. Y.; Chen, W. S.; Yu, S. H., Wood-Derived Ultrathin Carbon Nanofiber Aerogels. *Angew. Chem. Int. Ed. Engl.* **2018**, *57* (24), 7085-7090.
6. Lu, X.; Zeng, Y.; Yu, M.; Zhai, T.; Liang, C.; Xie, S.; Balogun, M. S.; Tong, Y., Oxygen-deficient hematite nanorods as high-performance and novel negative electrodes for flexible asymmetric supercapacitors. *Adv. Mater.* **2014**, *26* (19), 3148-55.
7. Wang, Y.; Liu, T.; Lin, X.; Chen, H.; Chen, S.; Jiang, Z.; Chen, Y.; Liu, J.; Huang, J.; Liu, M., Self-Templated Synthesis of Hierarchically Porous N-Doped Carbon Derived from Biomass for Supercapacitors. *ACS Sustainable Chem. Eng.* **2018**, *6* (11), 13932-13939.
8. Zilong, W.; Zhu, Z.; Qiu, J.; Yang, S., High performance flexible solid-state asymmetric supercapacitors from MnO₂/ZnO core-shell nanorods//specially reduced graphene oxide. *J. Mater. Chem. C* **2014**, *2* (7), 1331-1336.
9. Xiao, X.; Peng, X.; Jin, H.; Li, T.; Zhang, C.; Gao, B.; Hu, B.; Huo, K.; Zhou, J., Freestanding mesoporous VN/CNT hybrid electrodes for flexible all-solid-state supercapacitors. *Adv. Mater.* **2013**, *25* (36), 5091-7.
10. Xiao, K.; Ding, L. X.; Liu, G.; Chen, H.; Wang, S.; Wang, H., Freestanding, Hydrophilic Nitrogen-Doped Carbon Foams for Highly Compressible All Solid-State Supercapacitors. *Adv. Mater.* **2016**, *28* (28), 5997-6002.
11. Wang, G.; Wang, H.; Lu, X.; Ling, Y.; Yu, M.; Zhai, T.; Tong, Y.; Li, Y., Solid-state supercapacitor based on activated carbon cloths exhibits excellent rate capability. *Adv. Mater.* **2014**, *26* (17), 2676-82, 2615.
12. El-Kady, M. F.; Strong, V.; Dubin, S.; Kaner, R. B., Laser Scribing of High-Performance and Flexible Graphene-Based Electrochemical Capacitors. *Science* **2012**, *335* (6074), 1326-1330.
13. Xiao, X.; Li, T. Q.; Yang, P. H.; Gao, Y.; Jin, H. Y.; Ni, W. J.; Zhan, W. H.; Zhang, X. H.; Cao, Y. Z.; Zhong, J. W.; Gong, L.; Yen, W. C.; Mai, W. J.; Chen, J.; Huo, K. F.; Chueh, Y. L.; Wang, Z. L.; Zhou, J., Fiber-Based All-Solid-State Flexible

- Supercapacitors for Self-Powered Systems. *Acs Nano* **2012**, *6* (10), 9200-9206.
- 14. Sun, Y.; Sills, R. B.; Hu, X.; Seh, Z. W.; Xiao, X.; Xu, H.; Luo, W.; Jin, H.; Xin, Y.; Li, T.; Zhang, Z.; Zhou, J.; Cai, W.; Huang, Y.; Cui, Y., A Bamboo-Inspired Nanostructure Design for Flexible, Foldable, and Twistable Energy Storage Devices. *Nano Lett.* **2015**, *15* (6), 3899-3906.
 - 15. Zheng, Z.; Retana, M.; Hu, X.; Luna, R.; Ikuhara, Y. H.; Zhou, W., Three-Dimensional Cobalt Phosphide Nanowire Arrays as Negative Electrode Material for Flexible Solid-State Asymmetric Supercapacitors. *ACS Appl. Mater. Interfaces* **2017**, *9* (20), 16986-16994.
 - 16. Yang, P.; Ding, Y.; Lin, Z.; Chen, Z.; Li, Y.; Qiang, P.; Ebrahimi, M.; Mai, W.; Wong, C. P.; Wang, Z. L., Low-cost high-performance solid-state asymmetric supercapacitors based on MnO₂ nanowires and Fe₂O₃ nanotubes. *Nano Lett.* **2014**, *14* (2), 731-6.
 - 17. Feng, J. X.; Ye, S. H.; Lu, X. F.; Tong, Y. X.; Li, G. R., Asymmetric Paper Supercapacitor Based on Amorphous Porous Mn₃O₄ Negative Electrode and Ni(OH)₂ Positive Electrode: A Novel and High-Performance Flexible Electrochemical Energy Storage Device. *ACS Appl Mater Interfaces* **2015**, *7* (21), 11444-51.
 - 18. E. Raymundo-Pinero, F. Leroux, F. Beguin, *Adv. Mater.*, 2006, **18**, 1877-1882.
 - 19. D. W. Wang, F. Li, M. Liu, G. Q. Lu, H. M. Cheng, *Angew. Chem. Int. Ed.*, 2008, **47**, 373-376.
 - 20. J. Zhang, J. Jiang, H. Li, X. Zhao, *Energy Environ. Sci.*, 2011, **4**, 4009-4015.